J Mater Sci: Mater Electron (2012) 23:2005–2009
DOI 10.1007/s10854-012-0694-9

Structure and dielectric properties of $BaO–B_2O_3–ZnO–[(BaZr_{0.2}Ti_{0.80})O_3]_{0.85} - [(Ba_{0.70}Ca_{0.30})TiO_3]_{0.15}$ glass–ceramics for energy storage

Venkata Sreenivas Puli · Dhiren K. Pradhan · Ashok Kumar · R. S. Katiyar · Xiaofeng Su · C. M. Busta · M. Tomozawa · Douglas B. Chrisey

Received: 24 December 2011 / Accepted: 12 March 2012 / Published online: 30 March 2012

Abstract Alkali-free [0.10 BaO + 0.4 B_2O_3 + 0.5 ZnO], [0.3 BaO + 0.6 B_2O_3 + 0.1 ZnO] glass powder materials were mixed with $[(BaZr_{0.2}Ti_{0.80})O_3]_{0.85} - [(Ba_{0.70}Ca_{0.30})TiO_3]_{0.1}$—BZT–BCT ceramic materials for energy density storage capacitor applications. Calcined (1,250 °C/10 h) BZT–BCT ceramic powder materials were mixed with (15 wt. %) two different glass compositions of [0.10 BaO + 0.4 B_2O_3 + 0.5 ZnO], [0.3 BaO + 0.6 B_2O_3 + 0.1 ZnO] separately and were ground using low energy ball milling for 2 h at 400 rpm. The ball milled powders were made into discs having 13 mm diameter and 0.5 mm thickness using hydraulic press (2 ton) and sintered at 900 °C for 2 h. Both the compositions have shown dielectric breakdown field strength ~260, 280 kV/cm and energy density values ~1.118 and 0.50 J/cm^3.

1 Introduction

Glass powders are widely used in ceramic capacitors, barrier ribs, and dielectric layer for front and back panels in plasma display panels. These dielectric layers should have a low dielectric constant, high transparency, and high breakdown voltage breakdown voltage with reasonable thermal expansion coefficient [1]. Even though glass materials alone can have higher breakdown voltages, but still they posses low dielectric constant values. Glass mixed ceramic materials with high dielectric constant and high breakdown voltages are necessary to maintain higher energy storage density values. Glass–ceramic composites materials that are prepared using high dielectric constant ceramic phases scattered within high breakdown field strength glass phase materials. Materials which are simultaneously exhibiting high dielectric constant and high breakdown field strengths are strong candidates for high energy density capacitor applications [2]. Materials with pore free and fine grains are highly desirable in ferroelectric ceramic applications [3]. The ferroelectric glass–ceramic based on $PbTiO_3$ was first reported by Bergeron in 1961 [4]. Gorzkowski et al. [5] reported that barium strontium titanate (BST) a ferroelectric glass ceramic with high dielectric constant (ε − 1,000) and breakdown strength 800 kV/cm, did not result in exceptional energy density values (0.9 J/cm^3) which is due to dendrites and pore in the microstructure [5]. $Nb_2O_5–BaO–Na_2O–SiO_2$ Glass–ceramics were prepared by means of rapid quenching and controlled crystallization for high energy density storage capacitor devices, the theoretical energy density values reached up to 1.87 MJ/cm^3 [6]. Strontium barium niobate glass ceramics might be one the strong candidate materials for energy density applications, were prepared by melt-casting method followed by controlled crystallization, shown a breakdown voltage of 1,400 kV/cm and with an energy density value of 4 J/cm^3 [7]. Addition of $BaO–SiO_2–B_2O_3$ glass–BST ceramics improved the energy density values ~0.89 J/cm^3, when compared to the pure BST (0.37 J/cm^3) [8]. Puli et al. [9, 10], recently reported that pure BZT–BCT ceramics exhibited high energy density values ~7.48 J/cm^3, calculated using the formula $Ed = (\varepsilon_0 \varepsilon_r E_b^2)/2$ and measured value ~2.10 J/cm^3 from P-E hysteresis loop, due to high dielectric permittivity ~7,135, even though breakdown strength ~53 kV/cm is low. In the present work,

V. S. Puli (✉) · D. K. Pradhan · A. Kumar · R. S. Katiyar
Department of Physics and Institute for Functional Nano Materials, University of Puerto Rico, San Juan, Puerto Rico, PR 00936, USA
e-mail: pvsri123@gmail.com

X. Su · C. M. Busta · M. Tomozawa · D. B. Chrisey
Department of Materials Science and Engineering, Rensselaer Polytechnic Institute, Troy, NY, USA

higher dielectric permittivity of BZT–BCT ceramics with higher energy density (7.48 J/cm^3) motivated us to prepare alkaline free glass mixed ceramics to achieve improved energy storage density.

2 Experimental

Stoichiometric ratio of $BaCO_3$, $CaCO_3$, TiO_2, Zr_2O_3 powder ceramics were mixed for 2 h by adding isopropanol as milling media with zirconium ball in a low energy ball miller. BZT–BCT powders dried overnight were calcined at 1,250 °C for 10 h. Phase formation of the powder was checked by X-ray diffraction (XRD) technique, and later, crystallized BZT–BCT ceramic powder was mixed with two different alkali-free glass compositions [0.10 BaO + 0.4 B_2O_3 + 0.5 ZnO], [0.3 BaO + 0.6 B_2O_3 + 0.1 ZnO] separately (each of 15 wt. % of glass powder), and were again mixed for 2 h by adding isopropanol as milling media in a low energy ball miller. Glass–ceramic powder materials 0.85 $\{[(BaZr_{0.2}Ti_{0.80})O_3]_{0.85} - [(Ba_{0.70}Ca_{0.30})TiO_3]_{0.1}\}$ + 0.15 [0.10 BaO + 0.4 B_2O_3 + 0.5 ZnO]—BZCTG1, and 0.85 $\{[(BaZr_{0.2}Ti_{0.80})O_3]_{0.85} - [(Ba_{0.70}Ca_{0.30})TiO_3]_{0.1}\}$ + 0.15 [0.3 BaO + 0.6 B_2O_3 + 0.1 ZnO]—BZCTG2 were added with 4 % polyvinyl alcohol (PVA) as an organic binder to increase the strength of green pellets having 13 mm diameter and 0.5 mm thickness. Pellets were kept at 500 °C for 30 min for binder removal and then sintered at 900 °C for 2 h in a Carbolite furnace. The structural and surface morphology of the sintered pellets were analyzed by XRD using $CuK_\alpha = 1.54$ Å radiation, Raman spectroscopy and scanning electron microscopy (SEM), respectively. To measure dielectric properties, sintered discs were painted with silver on either side of the surfaces and were dried at 350 °C for 1 h for electrode formation.

Temperature-dependent dielectric properties were carried out with an Alfa impedance analyzer with fully computer interfaced novocontrol thermal stage in the temperature range of 273–400 K in a frequency limit of 100–1 MHz. Electrical breakdown voltage of the samples was measured at room temperature using Trek high voltage amplifier.

3 Results and discussion

The XRD patterns of the samples of alkali free glass [0.10 BaO + 0.4 B_2O_3 + 0.5 ZnO], [0.3 BaO + 0.6 B_2O_3 + 0.1 ZnO] mixed BZT–BCT ceramics sintered at 900 °C for 2 h are shown in Fig. 1a. The glass–ceramics with two main phases: the tetragonal BZT–BCT was indexed with (h k l) plane and the glass–ceramic phases were shown with asterisk symbol. Figure 1b shows SEM images of glass–ceramics (BZCTG1, BZCTG2) sintered at 900 °C for 2 h. SEM micrographs of discs revealed pore-free and dense surfaces. The average grain size of the glass mixed (BZCTG1, BZCTG2) ceramics pellets is between 5 and 10 microns with crystalline behavior. Unidentified pore might be one the reasons for low breakdown field strength of glass compositions. Local structure of the glass mixed ceramic BZT–BCT is identified with Raman spectroscopy, and is a powerful technique for the study of ferroelectric materials because of the close relationship between ferroelectricity and lattice dynamics [10]. Raman spectra of the sintered pellets were shown in the Fig. 2; the characteristic tetragonal perovskite structure Raman peaks were formed at the sintered temperature (900 °C for 2 h). Corresponding Raman peaks for the pure BZT–BCT ceramics were discussed in detail elsewhere [9]. Both glass–ceramic compositions (BZCTG1, BZCTG2) have shown the effective vibration modes: $3(A_1 + E) + E + B_1$ that are similar to BZT–BCT ceramics [9, 11]. Both A_1 and E modes further splits into longitudinal (LO) and transverse (TO) optical modes due to presence of long range electrostatic forces [12]. The weak E(TO) mode is observed at around

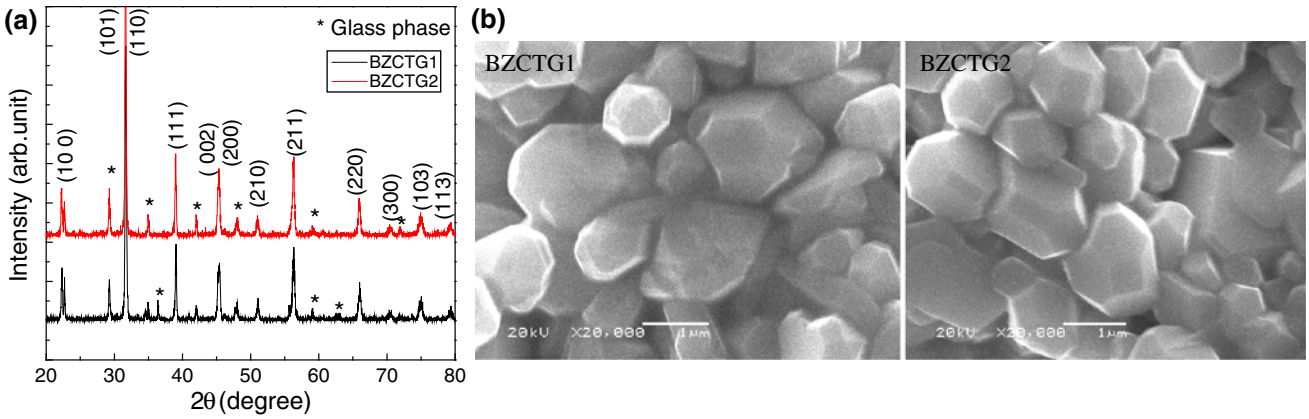

Fig. 1 Room temperature XRD patterns of glass–ceramics [0.10 BaO + 0.4 B_2O_3 + 0.5 ZnO], [0.3 BaO + 0.6 B_2O_3 + 0.1 ZnO] − $[(BaZr_{0.2}Ti_{0.80})O_3]_{1-x}$ − $[(Ba_{0.70}Ca_{0.30})TiO_3]_x$—BZCTG1, BZCTG2, sintered at 900 °C, with 2θ angle ranging from 10 to 80°

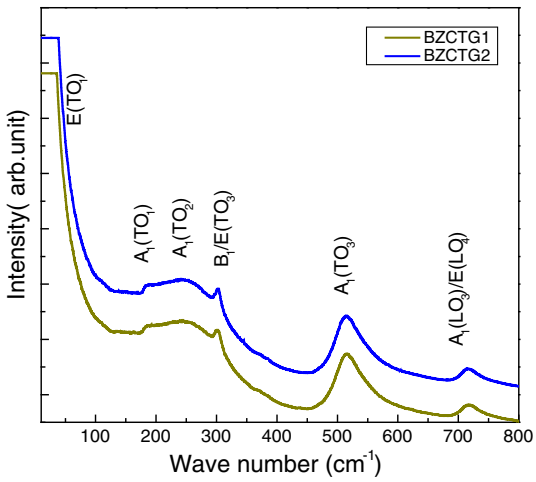

Fig. 2 SEM micrographs of glass–ceramics [0.10 BaO + 0.4 B_2O_3 + 0.5 ZnO], [0.3 BaO + 0.6 B_2O_3 + 0.1 ZnO] − $[(BaZr_{0.2}Ti_{0.80})O_3]_{1-x}$ − $[(Ba_{0.70}Ca_{0.30})TiO_3]_x$—BZCTG1, BZCTG2, sintered at 900 °C

$\sim$55 cm^{-1}, which was also observed in the pure BZT–BCT at lower Raman shift $\sim$37 cm^{-1} [9, 11]. The characteristic interference of the sharp A_1(TO) mode approximately (270 cm^{-1}) with the 180 cm^{-1} A_1(TO) mode in the pure $BaTiO_3$ ceramic is due to the coupling between A_1 modes, and it results in an anti-resonance effect at $\sim$180 cm^{-1} and these peaks along with A_1(LO)/E(TO) modes indicate the tetragonal crystal structure for pure $BaTiO_3$ ceramics [13]. For present glass mixed BZT–BCT ceramics, the $A_1(TO_1)$ anti-symmetry mode detected at $\sim$170–173 cm^{-1} shifted towards higher frequencies. The anti-symmetry mode $A_1(TO_2)$ between 240 and 242 cm^{-1} is also shifted towards the higher frequency regions and which are ascribed due to the asymmetric Ti–O phonon vibrations. $E(TO_3)/B_1$ mode is also one of the characteristic tetragonal symmetry mode for pure $BaTiO_3$ at around $\sim$301–303 cm^{-1}, where as the broad and asymmetric $E(TO_3)/B_1$ mode observed at around 290–292 cm^{-1} for present BZT–BCT is shifted to lower frequency region as the Ca content increased and as well Zr content decreased, which are ascribed due to the asymmetric Ti–O phonon vibrations and as well as this is also related to the lowering of ferroelectric phase transition Curie temperature. The A_1 (TO_3) mode is observed at around 515 cm^{-1} is due to O–Ti–O symmetric stretching vibrations [14]. These modes correspond to higher concentrations of polar $[TiO_6]$ octahedral, tetragonally distorted clusters in an overall cubic matrix of $Ba(Zr_{0.25}Ti_{0.75})O_3$; the E(TO + LO) mode is particularly symptomatic of the existence of polar

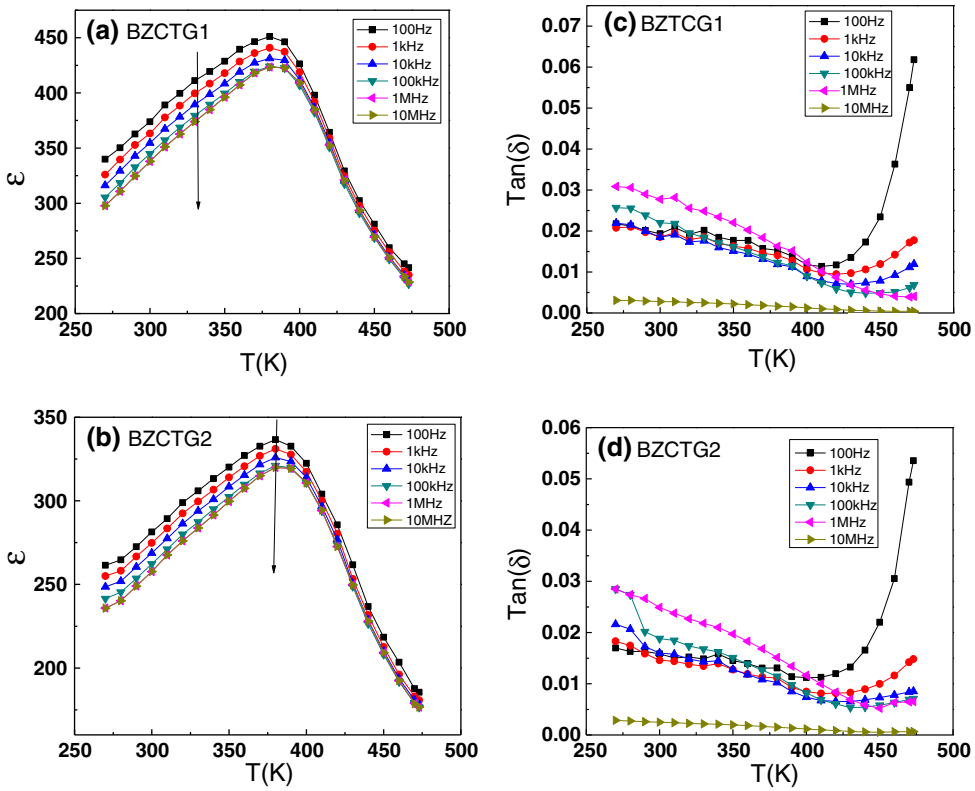

Fig. 3 **a**, **b** The temperature dependence of the dielectric permittivity of glass–ceramics [0.10 BaO + 0.4 B_2O_3 + 0.5 ZnO], [0.3 BaO + 0.6 B_2O_3 + 0.1 ZnO] − $[(BaZr_{0.2}Ti_{0.80})O_3]_{1-x}$ − $[(Ba_{0.70}Ca_{0.30})TiO_3]_x$—BZCTG1, BZCTG2, sintered at 900 °C at 100–1 MHz. **c**, **d** The temperature dependence of the dielectric loss (tan δ) of glass–ceramics [0.10 BaO + 0.4 B_2O_3 + 0.5 ZnO], [0.3 BaO + 0.6 B_2O_3 + 0.1 ZnO] − $[(BaZr_{0.2}Ti_{0.80})O_3]_{1-x}$ − $[(Ba_{0.70}Ca_{0.30})TiO_3]_x$—BZCTG1, BZCTG2 sintered at 900 °C at 100–1 MHz

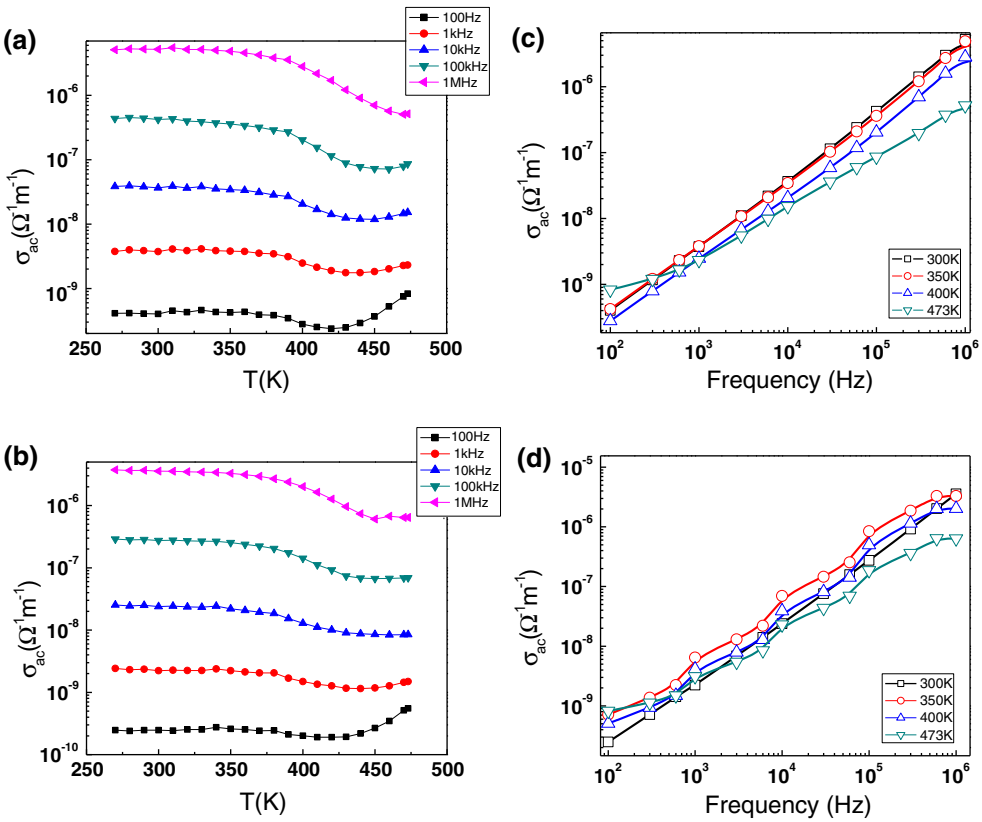

Fig. 4 **a**, **b** Ac conductivity (σ_{ac}) as a function of temperature and **c**, **d** Ac conductivity (σ_{ac}) as a function of frequency at different temperature (300, 350, 400, 473 K) of glass–ceramics [0.10 BaO + 0.4 B_2O_3 + 0.5 ZnO], [0.3 BaO + 0.6 B_2O_3 + 0.1 ZnO] − $[(BaZr_{0.2}Ti_{0.80})O_3]_{1-x}$ − $[(Ba_{0.70}Ca_{0.30})TiO_3]_x$—BZCTG1, BZCTG2 sintered at 900 °C at 100–1 MHz

Table 1 Dielectric permittivity, dielectric loss, breakdown field strength, and energy storage density of glass–ceramics [0.10 BaO + 0.4 B_2O_3 + 0.5ZnO], [0.3 BaO + 0.6 B_2O_3 + 0.1ZnO] − $[(BaZr_{0.2}Ti_{0.80})O_3]_{1-x}$ − $[(Ba_{0.70}Ca_{0.30})TiO_3]_x$—BZCTG1, BZCTG2 sintered at 900 °C at 100–1 MHz

Compound	Dielectric permittivity (25 °C)	Breakdown voltage (V)	Breakdown field (kV/cm)	Energy density (J/cm^3)
$0.85\{[(BaZr_{0.2}Ti_{0.80})O_3]_{0.85} - [(Ba_{0.70}Ca_{0.30})TiO_3]_{0.1}\} + 0.15$ [0.10 BaO + 0.4 B_2O_3 + 0.5 ZnO]	378	13,000	260	1.118
$0.85\{[(BaZr_{0.2}Ti_{0.80})O_3]_{0.85} - [(Ba_{0.70}Ca_{0.30})TiO_3]_{0.1}\} + 0.15$ [0.3 BaO + 0.6 B_2O_3 + 0.1 ZnO]	272	14,000	280	0.50

$[TiO_6]$ clusters in a perovskite structure [15]. Polar $[ZrO_6]$ and especially $[TiO_6]$ clusters are responsible for the mode $A_1(LO_3)$/E(LO) observed at around 714–716 cm^{-1} [12]. The E(TO) mode also shifts towards lower frequency region with increase in Ca percentage, due to small grain sizes and stress affects the sample exhibit broadening and shifting of Raman modes. There is no evidence of the A_{1g} octahedral breathing mode around ~800 cm^{-1} in the characteristic spectra of BZT–BCT [11, 12].

Figure 3a, b shows the temperature dependent dielectric permittivity of glass mixed BZT–BCT ceramic composites at 100 Hz–10 MHz frequency. Temperature dependent dielectric permittivity curves exhibit a broad dielectric anomaly at all the frequency regions. As the temperature increased, dielectric permittivity values increased gradually up to 380 K and then decreased. Different amounts of glass–ceramic composites (BZCTG1, BZCTG2) exhibited room temperature dielectric permittivity values of ε ~378, ~272 respectively. Pure BZT–BCT compositions synthesized using solid state route and sol–gel route exhibit higher room temperature permittivity values ε ~7,135, ~1,248 [11, 12]. Glass addition might be the obvious reason for the decrease in dielectric permittivity values for glass–ceramic composites. Both compositions of glass–ceramic composites exhibited low dielectric loss values as shown in the Fig. 3c, d. At room temperature BZCTG1 shown low dielectric loss at ~0.01 and BZCTG2 shown a loss of 0.15 in the frequency region 100 Hz-10 MHz. As the temperature increased from 270 to 450 K there is a gradual decrease in dielectric loss and then started increasing till the measured temperature (475 K). Temperature dependence of conductivity (σ_{ac}) is shown in the

Fig. 4a, b for glass–ceramics (BZCTG1, BZCTG2). As the temperature increased from 273 to 450 K, conductivity (σ_{ac}) maintained almost constant conducting behavior till 400 K and then slowly conductivity increased for higher temperatures throughout the entire frequency range (100–1 MHz). Higher conducting behavior is from observed at 100 Hz and as the frequency reached 1 MHz whose conductivity decreased drastically. The resistivity of the samples (BZCTG1, BZCTG2) is fairly high at low temperatures. Low conductivity values were observed for both (BZCTG1, BZCTG2) glass–ceramics to that of their BZT–BCT ceramic counterpart [9, 11]. Linear behavior is observed in frequency dependence conductivity (σ_{ac}) is shown in the Fig. 4c, d for glass–ceramics (BZCTG1, BZCTG2). As the frequency increased from 100 Hz to 1 M Hz, very low conductivity values were observed in low frequency region and then conductivity continuously increased for higher frequency region at selected temperatures (300 K, 350 K, 400 K, and 473 K). Glass–ceramic composites (BZCTG1, BZCTG2) were completely crystallized at 900 °C, crystallized pellets with 0.5 mm thickness, were immersed in HT 200 oil to test the dielectric breakdown voltage. Room temperature dielectric permittivity, electrical breakdown field and energy density storage capacity were shown in the table. As the glass composition changed from BZCTG1 to that of BZCTG2, dielectric permittivity decreased from $\varepsilon \sim 378$ to 272, whereas, electrical breakdown field values are increased from 260 kV/cm to 280 kV/cm. The energy storage density values were calculated using the formula, $E_d = (\varepsilon_0\, \varepsilon_r\, E_b^2)/2$, where E_d is the energy storage density (J/cm^3), ε_0 is the permittivity of free space (8.85×10^{-14} F/cm), ε_r is the relative permittivity. The calculated energy storage density values are also tabulated in Table 1, even though the dielectric breakdown fields are moderately higher than the pure ceramic BZT–BCT (electric breakdown field ~ 153 kV/cm and energy density ~ 7.48 J/cm^3) calculated using the above formula $E_d = (\varepsilon_0\, \varepsilon_r\, E_b^2)/2$ and measured value ~ 2.10 J/cm^3 from P-E hysteresis loop) [9–11], whose energy storage density values are considerably low (1.118, 0.5 J/cm^3), which is due to lowest room temperature dielectric permittivity values due to addition of alkali free glass.

4 Conclusions

The electric breakdown field strength of glass–ceramics (BZCTG1, BZCTG2) are 260, 280 kV/cm and energy density values are ~ 1.118 and 0.50 J/cm^3 respectively. Though the break down strength of present samples is moderately higher and their energy storage densities are comparably low due to low room temperature dielectric permittivity values. Higher breakdown strength and low loss might be due the presence of alkali free glass composition and low loss dielectric BZT–BCT ceramic composition. The glass–ceramic composites have shown better dielectric breakdown field but low energy density compare to parent ceramics.

Acknowledgments This work was supported by the NSF award grant #1038272. The authors are also thankful to Cristina Diaz Borrero, Material Characterization Center, University of Puerto Rico for doing SEM measurements.

References

1. Seung Kwon Hong, Hye Young Koo, Dae Soo Jung, II Soon Suh, Yun Chan Kang, J. Alloys Compd. **437**, 215–219 (2007)
2. A. Herczog, IEEE Trans. PHP **9**(4), 247–256 (1973)
3. S.M. Lynch, J.E. Shelby, J. Am. Ceram. Soc. **61**(6), 424–427 (1978)
4. C.G. Bereeron, in *Crystallization of Perovskite Lead Titanate from Glasses*. Ph.D. thesis. University of Illinois, Urbana (1961)
5. E.P. Gorzkowski, P. Ming-Jen, A.B. Barry, C.M.W. Carl, J. Am. Ceram. Soc. **91**(4), 1065–1069 (2008)
6. M. Changhui, S. Xudong, D. Jun, T. Qun, J. Phys. Conf. Ser. **152**, 012061 (2009)
7. H.C. Guo, J.Z. Wen, Adv. Mater. Res. **311–313**, 2071–2074 (2011)
8. Z. Qingmeng, W. Lei, L. Jun, T. Qun, D. Jun, J. Am. Ceram. Soc. **92**(8), 1871–1873 (2009)
9. V.S. Puli, D.K. Pradhan, A. Kumar, D.B. Chrisey, M. Tomozawa, S.K. Ram, Mater. Res. Bull. (under review)
10. V.S. Puli, A. Kumar, R.S. Katiyar, X. Su, C.M. Busta, D.B. Chrisey, M. Tomozawa, J. Non Crystall. Solids (under review)
11. V.S. Puli, A. Kumar, D.B. Chrisey, M. Tomozawa, J.F. Scott, S.K. Ram, J. Phys. D Appl. Phys. **44**, 395403 (2011)
12. W. Min, Z. Ruzhong, Q. Shishun, L. Longdong, J. Mater. Sci. Mater. Electron. **23**(3), 753–757 (2011)
13. A. Chaves, R.S. Katiyar, S.P.S. Proto, Phys. Rev. B **10**, 3523–3533 (1974)
14. J.C. Sczancoski, L.S. Cavalcante, T. Badapanda, S.K. Rout, S. Panigrahi, V.R. Mastelaro, J.A. Varela, M.S. Li, E. Longo, Solid State Sci. **12**, 1160–1167 (2010)
15. A. Dixit, S.B. Majumder, R.S. Katiyar, J. Mater. Sci. **41**, 87–96 (2006)